Experimental investigation of a dielectric liquid-vapor interface between two vertical planar electrodes: Influence of the DC electric field and temperature

Baptiste Blaineau, Sébastien Dutour, Thierry Callegari, Pascal Lavieille, Marc Miscevic, Stéphane Blanco, Benoît Schlegel, Yves Bertin, Adel Benselama

Experimental investigation of a dielectric liquid-vapor interface between two vertical planar electrodes: influence of the DC electric field and temperature.

Baptiste BLAINEAU[a], Sébastien DUTOUR[a,*], Thierry CALLEGARI[a], Pascal LAVIEILLE[a], Marc MISCEVIC[a], Stéphane BLANCO[a], Benoit SCHLEGEL[a], Yves BERTIN[b], Adel M. BENSELAMA[b]

[a] *Université de Toulouse ; UPS, INP, CNRS ; LAPLACE (Laboratoire Plasma et Conversion d'Energie) ; 118 route de Narbonne, F-31062 Toulouse, France*
[b] *Insitut Pprime CNRS-ENSMA-Université de Poitiers, ENSMA, 1 avenue Clément Ader BP 40109, F-86961 Futuroscope Chasseneuil Cedex, France*

Abstract

The effect of a DC electric field on a liquid-vapor interface was investigated at different temperatures using a Pellat-like test cell filled with HFE-7000 and HFE-7100 dielectric fluids. Special attention was given to the local observations of the meniscus as this information is crucial in two-phase heat transfer applications. The results confirmed first that the dielectrophoretic force controls both the mean position and the shape of the meniscus as the visualizations revealed that the interface could be totally flattened when the electric field increased. The visualizations showed secondly that free charges in the liquid could affect the interface behavior in two ways: by slightly modifying the pressure profile in the liquid bulk, and by leading the formation of electrojets close to the wall. The temperature dependence of the vapor dielectric strength led to a drastic limitation at low temperature of the maximum electric field that the fluid could withstand before breakdown. This point should be carefully considered in electrohydrodynamics enhanced two-phase cooling systems.

Keywords: Liquid-vapor interface, Electrohydrodynamics, Two-phase cooling systems

1. Introduction

Heat pipes, Capillary Pumped Loops (CPL) and Loop Heat Pipes (LHP) are passive two-phase systems which are involved in electronics cooling. The vaporization of the working fluid in a porous wick or sub-millimeter grooves results in a natural fluid circulation between the heat exchangers. These devices are highly efficient and reliable. However, the maximum heat load transferred by the cooling system is mainly restricted by the maximum pumping capability of the capillary structure which is given by the maximum pressure difference generated at the vaporisation interface (the capillary limit). In order to improve the performance of such cooling systems, it is now considered to assist them with an active device supplying power to the fluid. One option is to use an electric field and the electrohydrodynamic (EHD) forces induced in the fluid. Actually, within this approach, the power consumption is very low compared to mechanical pumping and no moving pieces are involved reducing the risk of failure.

The use of an electric field in order to enhance the performance of the capillary systems has been considered since the seventies and was firstly motivated by space applications [1], [2], [3]. The approach considered that the capillary structure of heat pipes might be augmented or replaced by electrodes and EHD pumping. Equivalent thermal performance of conventional axial-groove heat pipes was achieved but questions regarding the long-term stability of dielectric fluids in the presence of corona and intermittent discharges drastically restrained their development.

Later on, Babin et al. [4] coupled an ion-drag pump with a small CPL filled with $R11$ fluid. The approach was slightly different than previously because the electrodes could be placed in the liquid line of the capillary pump. Here, unipolar charges were injected by a set of needles to overcome the pressure drop in the loop. The comparison of performance in a horizontal orientation with and without the ion-drag pump showed an enhancement of 20% to 60% of the heat transport capacity. Once the conduction regime based on the dissociation of the liquid molecules into ions has been clarified [5], the investigation became more active as a longer stability of the liquid properties can be expected. A determinant effort was the fact of J. Yagoobi and his co-workers who demonstrated a 100% enhancement in the transport capacity of a monogroove heat pipe [6], [7]. They also investigated two-phase cooling systems based on the pumping of millimetric liquid films [8], [9]. An important demonstration for the potential of conduction pumping at a larger scale was due to Jeong et al. [10], [11] who tested a ten-meters long two-phase loop filled with $R134a$. They found that for an applied voltage of 15 kV and a sink temperature of $20°C$, the generated pressure head was approximately 9.6 kPa and the transported heat load reached 130 W.

A somewhat different approach was provided by Mo et al. [12], [13] who investigated a larger CPL (maximum allowable heat-transport capacity of 1 500 W) filled with $R134a$ and involving a EHD-assisted cylindrical evaporator. Here, a spring electrode was inserted under the wick within the evaporator

*Corresponding author
Email address: sebastien.dutour@laplace.univ-tlse.fr (Sébastien DUTOUR)

core while the casing was grounded in order to influence the liquid-vapor separation inside the evaporator and to assist the pumping menisci in the wick. The results showed that up to three times heat-transfer coefficient enhancement could be obtained. They also revealed that the deprime condition of a capillary pump can be prevented in the presence of an electric field. Harvel et al. [14] confirmed a significant decrease of the partial dry out mechanism of the evaporator using a coaxial electrode directly located in the evaporator core.

Concurrently to pumping, EHD has been widely used with the objective of the two-phase heat transfer enhancement. Up to 20 times of augmentation of the average heat transfer coefficient was reported in the existing literature as compiled by Laohalertdecha et al. [15]. A recent example of application to a gravity heat pipe filled with HFE-7000 and using AC electric field in the evaporator is proposed by Smith et al. [16]. A cylindrical electrode was inserted along the thermosyphon axis whilst the casing was grounded. They found an enhancement up to 40% of the evaporator heat transfer coefficient for heat flux lower than $8\,kW/m^2$ due to the the thinning of the liquid film in contact with the evaporator wall. But, the electric field also led to a partial dry-out of the evaporator for greater heat flux.

These numerous demonstrations of a significant improvement in the performance of two-phase cooling systems contrast with the fact that, to our knowledge, none of these devices has been implemented in thermal management applications. This is primarily due to some technical issues: (i) charge injection at the surface electrode leads to a fast alteration of both electrodes and fluid properties so it must be avoided; as this regime is highly affected by the wall shape and its surface state, the design of the electrodes and their integration in the cooling system remain extremely sensitive, (ii) the implementation of EHD devices with high voltage is difficult with some widely used fluids which are highly conductive such as water and ammonia. In this case, an electrode coating with a dielectric layer is necessary to limit the current; defaults in this coating can breakdown at relatively low voltages limiting the operating range. Another limitation is the high complexity of the phenomena involving different electrostatic effects, fluid flow, interface dynamics and instabilities, temperature gradients and heat flux. This is indeed demanding for theoretical investigations and numerical efforts with the objective of the cooling system dimensioning. In addition, there is still a lack of understanding of some observations especially in the interfacial region. For instance, the origin of the saturation of the contact angle in electrowetting on dielectric remains an open question [17].

Facing this, there is a serious need of investigations that report carefully designed experiments in simple geometric configurations with the objectives to analyze the influence of temperature and heat transfer as encountered in operating conditions of the cooling systems. Thus, we propose to study the behavior of a two-phase dielectric fluid confined between two vertical and parallel electrodes. This configuration, which actually corresponds to the original work of Pellat [18], has many advantages: it is an experiment commonly used to understand different well controlled problems and we thus benefit of some studies clarifying separately the electrical conduction in the liquid [5], the electrowetting phenomenon at the wall [19], [20] and some effects of surface tension [21]. Then, it offers a simple way to control the heating of the fluid from above the interface or directly through the liquid zone. In measuring the liquid height-of-rise, it is possible to determine the global force acting on the liquid column. Additionally, in observing the interface shape and dynamics, a more local information can be achieved and this is determinant for heat transfer specially close to the wall. The objective is firstly to study the interface behavior when a DC electric field strength is increased and, in a second hand, to determine the influence of the temperature based on some isothermal observations performed at different temperatures.

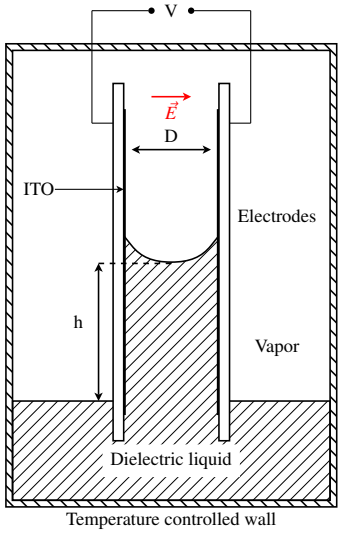

Figure 1: Test cell configuration and schematic end-of-view of the meniscus.

2. Background

The electrical force acting on a fluid is usually formulated in terms of the Korteweg-Helmoltz body force density:

$$\mathbf{f} = q\,\mathbf{E} - \frac{E^2}{2}\nabla\varepsilon + \frac{1}{2}\nabla\left[\rho\left(\frac{\partial\varepsilon}{\partial\rho}\right)_T E^2\right] \qquad (1)$$

where q is the volume density of free charge, $\mathbf{E}$ the electric field, ρ the mass density and ε is the permittivity which is assumed to be a function of the mass density and temperature.

The first term is the Coulomb's force. In a dielectric fluid, free charges can have two different sources. Firstly, they can be created by dissociation/recombination of the fluid molecules into ions with an opposite charge. Secondly, at larger electric field, charges could come from injection at the electrode-fluid interface where an electron is exchanged between the electrode metal and a molecule of the liquid.

The two last terms of the equation (1) which are respectively the dielectrophoretic (DEP) force and the electrostriction force are due to the polarization of the fluid with the electric field. In a

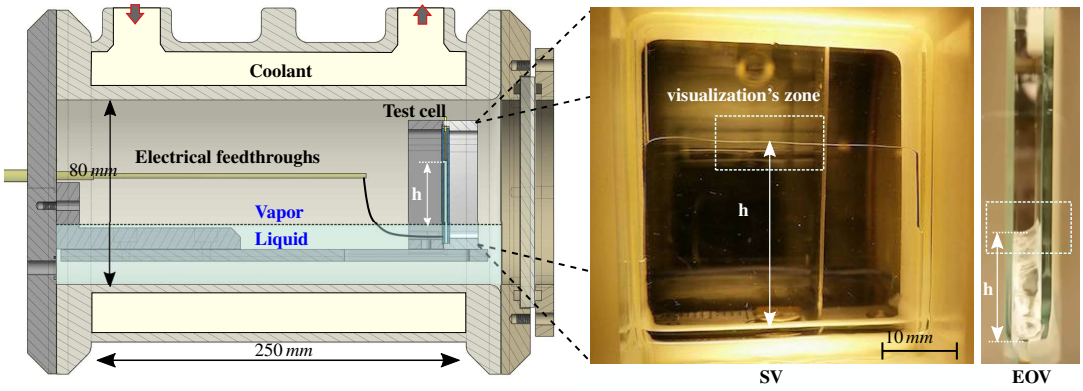

Figure 2: Test cell in its enclosure and view points of the liquid height-of-rise (SV: side-view; EOV: end-on view).

two-phase system, the polarization forces act principally in the liquid-vapor interfacial zone where there is an important variation of the permittivity with the fluid mass density. Moreover, the literature converges to the suggestion that electrostriction has no observable influence on the incompressible electrohydrostatics [20].

3. Experimental set-up and fluids properties

3.1. Experimental set-up

The test cell is based on the Pellat's original experiment: two vertical planar electrodes are partially immersed in the liquid (figure 1). The electrodes are made of a 1 *mm*-thick plates of glass coated with indium tin oxide (ITO). The conductive layer has a height of 40 *mm* and a width of 30 *mm*. The spacing between the plates D can be set to 2.03 *mm* and 3.02 *mm* using glass rods which are placed horizontally at the bottom and at the top of the electrodes so that the liquid is free to fall and flow on the side. The experiment takes place within an enclosure made of a double casing glass cylinder in which a transparent coolant circulates at controlled temperature (figure 2). On one end, a disk made of sapphire is placed in order to perform the interface visualizations and also IR measurements. The test cell can be placed with the electrodes pair either parallel or perpendicular to the viewport providing respectively a side-view or an end-on view of the liquid height-of-rise.

The experimental procedure consisted in increasing the voltage by steps of 0.25 *kV* of the high voltage (HV) electrode while the other electrode was grounded. A simultaneous high-speed video camera capture was used to determine the mean liquid height-of-rise h and the end-of-view interface shape and dynamics. As the electrodes formed an opened channel, the liquid fell out by the side and a lateral motion was observable. Nevertheless, a large unperturbed zone existed in the center of the cell where the interface was stable. The observations focussed on this region. The image resolution was 35 pixels/mm and the recording was set at 4 000 frames/s. The maximum voltage of each of the series was achieved either when the liquid reached the top of the electrodes or just before the breakdown limit in the covering vapor was reached. The maximum temperature for each fluid was fixed by the maximum pressure allowed by the enclosure (2 *bar*). Actually, following the temperature modification, the pressure changed from 0.24 *bar* at 2°*C* to 2.2 *bar* at 60°*C* for the HFE-7000 and from 0.10 *bar* at 2°*C* to 1.8 *bar* at 80°*C* for the HFE-7100.

For a given fluid sample and a given pair of electrodes, the repeatability of the height-of-rise measurements was established on a test during which the steps amplitude (increasing or decreasing steps, small and large amplitudes), the time duration before another step were changed. We found that the deviations were always lower than ±2 *mm*. The experiments were performed both at $D = 2.03$ *mm* and at $D = 3.02$ *mm*. No significative influence of the inter-electrodes spacing were found on the results even though the deviations were more noticeable for HFE-7100.

3.2. Liquid phase properties

The working HFE fluids are dielectric fluids with low global warming potential that have been developed for thermal management applications. The purity was 99.5%. In order to remove non-condensable gases, the fluids were preliminarily boiled in a separated device while high vacuum was reached in the test cell before filling. Then, the fluid saturation was controlled in situ by comparing the saturation temperature obtained from the pressure measurement with the fluid temperature. Some additional physical properties at 25°*C* are given in table 1.

	HFE-7000	**HFE-7100**
Liquid mass density $[kg/m^3]$	1400	1510
Surface tension $[mN/m]$	12.4	13.6
Dielectric constant	7.4	7.4
Electrical conductivity $[S/m]$	$1 \cdot 10^{-6}$	$3 \cdot 10^{-8}$

Table 1: HFE liquid properties at 25 °C from 3M data-sheets.

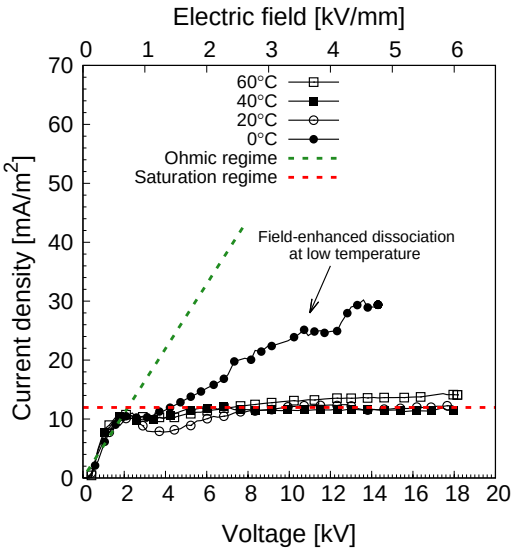

(a) for HFE-7000.

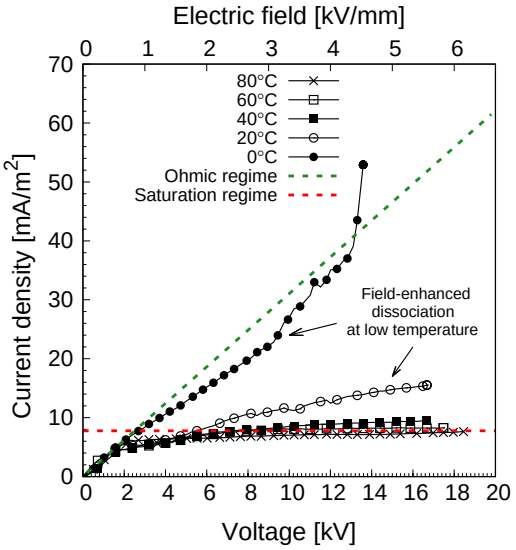

(b) for HFE-7100.

Figure 3: Current density versus the voltage and the electric field at different temperatures.

In order to investigate qualitatively the electrical conduction in both liquids, some dedicated experiments were made with the inter-electrodes spacing entirely filled with liquid. Figure 3 shows the current density in both liquids as a function of the voltage and the mean electrical field at different temperatures. The quasi-ohmic regime was observable below $2\,kV$. Then, for a given temperature, the curves deviated from a linear voltage dependence which is typical to the dissociation/recombination regime and (i) at high temperature, the current became almost constant and the saturation regime was reached; (ii) at low temperature, the current still increased with the voltage but with a different rate. This latter behavior is representative of the field-enhanced ionic dissociation regime. As predicted by Onsager [22], the dissociation rate is greater at low temperature for a given electrical strength.

In the ohmic regime, the ratio current density to the electric field j/E gives an order of magnitude of the electrical conduction in the device. For the HFE-7100, this ratio $j/E \approx 0.93\,10^{-8} S/m$ is consistent both with the electrical conductivity provided in table 1 and with the measurements performed by [23]. For HFE-7000, $j/E \approx 1.65\,10^{-8} S/m$ which is two orders of magnitude lower than the 3M value. Surprisingly, no reference measurements are available in the literature for this fluid. However, based on the results obtained for HFE-7100, we could reasonably suggest that the electrical conductivity provided by 3M for the HFE-7000 may not be accurate. Obviously, this statement has to be confirmed by some specific measurements.

4. Results and discussion

4.1. The DEP force and the liquid height-of-rise

Figure 4 shows the liquid column height-of-rise h versus the electric field for both fluids and for temperatures ranging from $0°C$ to $80°C$. A secondary axis was built by multiplying the h-axis by a constant liquid density (see table 1) with the objective to give an estimation of the hydrostatic pressure. Actually, this value deviated from 4% (underestimation) at the minimum temperature to 10% (overestimation) at the maximum temperature. For HFE-7000, the deviation was about ±4%.

The electric field dependency of h is a square law and the data are consistent with the dielectric height-of-rise h_{DEP}. This suggests that the DEP force is dominant as h_{DEP} is defined by [20] in a perfectly insulating fluid taking into account the DEP force only:

$$h_{DEP} = \frac{\frac{1}{2}\varepsilon_0 \left(\varepsilon_r - 1\right) E^2}{\rho_l\, g} \tag{2}$$

where the electric field is assumed to be $E = V/D$ along a surface enclosing the interface entirely. The variation with temperature of the liquid dielectric constant ε_r was estimated using the temperature dependent expressions for the mass density provided by Rausch et al. [24] and the Clausius-Mossotti relation:

$$\left(\frac{\varepsilon_r - 1}{\varepsilon_r + 2}\right)\frac{1}{\rho_l} = const \tag{3}$$

where the constant was determined using the data given in table 1. Based on this approach, the liquid dielectric constant decreased with temperature in a quasi-linear trend. This is consistent with [23] for HFE-7100 even though their results were slightly lower (8% to 10%).

The effect of temperature is shown in more details in Figure 5 for several electric field strengths. The breakdown limit curve gives the maximum field strength for which a height-of-rise could be maintained without the vapor became conductive. For both fluids, h was not really affected by the temperature in the range of investigation. The larger discrepancies (about $4\,mm$) with the dielectric height-of-rise were observed for HFE-7100, (i) when $E \leq 3.1\,kV/mm$ within an intermediate temperature range from $30°C$ to $60°C$ and (ii), when the field was greater

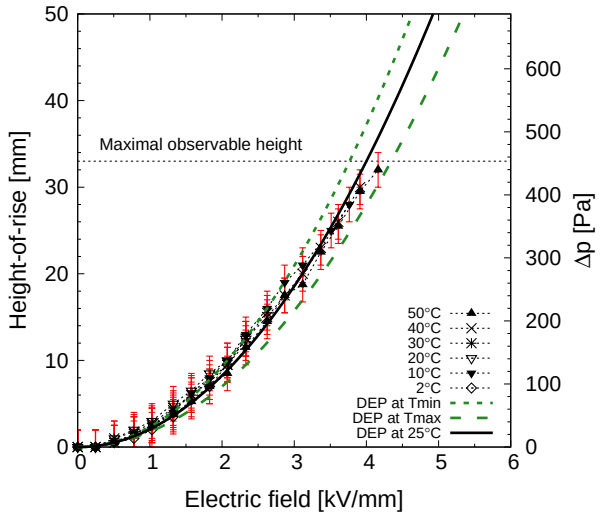

(a) for HFE-7000.

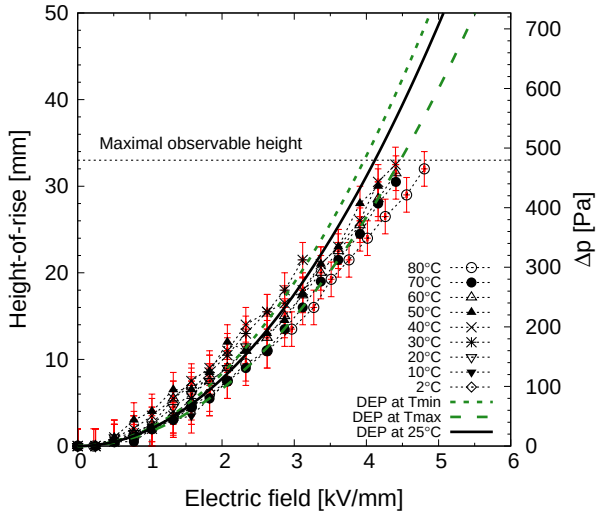

(b) for HFE-7100.

Figure 4: Liquid height-of-rise versus the electric field for (a) HFE-7000 and (b) HFE-7100 at different temperatures. DEP labelled curves correspond to equation (2) predictions.

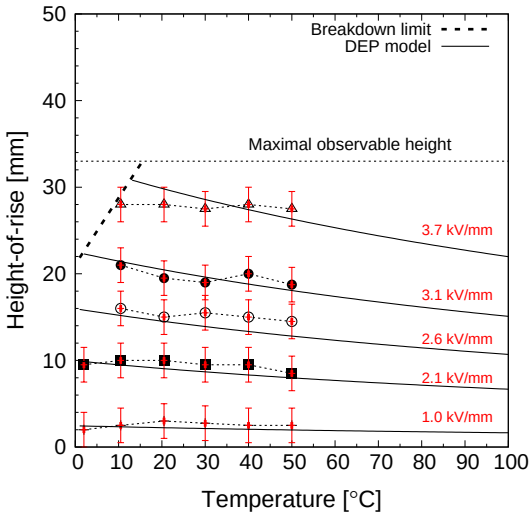

(a) for HFE-7000.

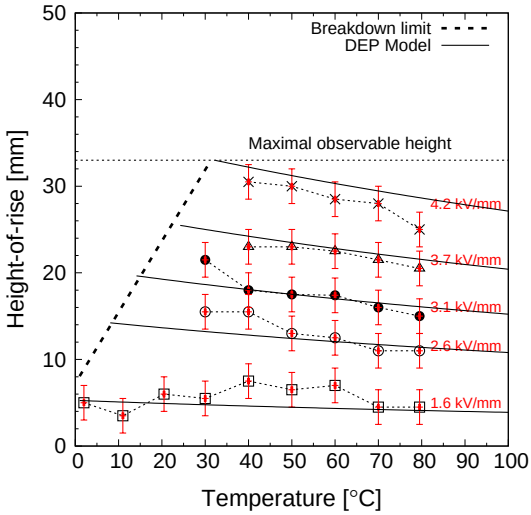

(b) for HFE-7100.

Figure 5: Liquid height-of-rise versus the temperature for (a) HFE-7000 and (b) HFE-7100 and for different electric field strengths.

than 4.2 kV/mm. The latter case corresponded to the more intense fluid circulation through the electrodes spacing and then the interface rise may be slightly limited by the pressure drop in the liquid. In the first case, the electrical conduction in the liquid could be a reason, as it is discussed in the next section. However, except for these few values, the data compared quite satisfactorily with the dielectric model prediction and then, according to equations (2) and (3), the rather weak effect of temperature could be correlated to the decrease of the dielectric constant.

Finally, the main influence of the temperature was given by the extension of the vapor breakdown domain. Actually, a drastic limitation of the operating range was observed with the decrease of the temperature. The most concerned fluid was HFE-7100. For instance, the hydrostatic pressure was limited at 100 Pa ($h \approx 5\,mm$) at 0°C while it could exceed 500 Pa ($h \approx 30\,mm$) at 40°C. The breakdown limit is mainly influenced by the vapor pressure: the lower the pressure, the lower the voltage threshold (except at extremely low pressure where the breakdown field strength increase again). This behavior was consistent with the observations as the lowest vapor pressure was achieved for HFE-7100.

4.2. Effect of the electrical conduction in the liquid

Figure 6 shows the influence of the electric field on the shape of the interface for a temperature of 60°C and for HFE-7100. When no voltage was applied, the end-on view exhibited an interface profile that was symmetric and curved by capillary

effect. As the electric field was increased, the meniscus first remained curved but became more and more asymmetrical. The liquid accumulated on the HV electrode and the meniscus rose for almost $2\,mm$ higher than in the opposite side at $E = 1.39\,kV/mm$. Then, it started to become smoother and smoother and finally the interface was maintained totally flat beyond $E = 2.79\,kV/mm$. A similar behavior was observed for HFE-7000 even though the asymmetry was less pronounced.

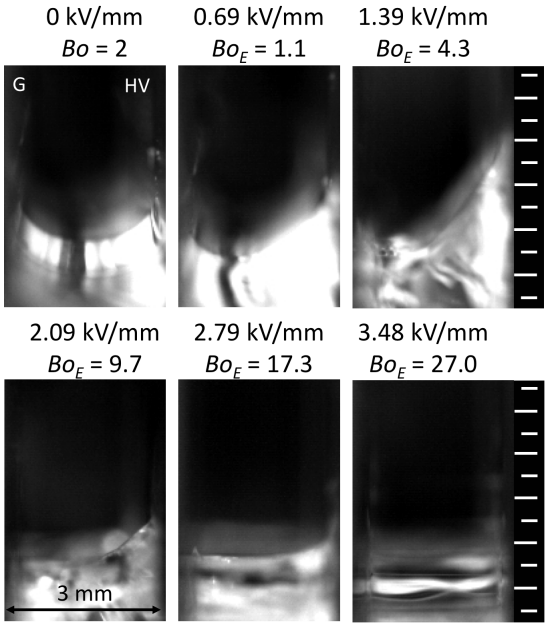

Figure 6: Influence of the electric field on the shape of the interface for a temperature of 60 °C and for HFE-7100; high voltage was applied on the right-hand side electrode.

As it is nearly close to zero, the contact angle is not affected by the EHD forces so that the interface profile behavior results from gravitational, surface tension and electrical forces. The relative importance of each term can be measured using dimensionless numbers such as the Bond number Bo and the dielectric Bond number Bo_E defined by:

$$Bo_E = \frac{\frac{1}{2}(\varepsilon_l - \varepsilon_0)E^2}{\frac{2\gamma}{D}} = \frac{(\varepsilon_l - \varepsilon_0)E^2 D}{4\gamma} \tag{4}$$

The Bo number gives the relative importance of gravity and surface tension: the capillary force is dominant when $Bo \ll 1$. In a similar way, the Bo_E number compares the DEP force with surface tension. The ratio Bo_E/Bo corresponds to the electrogravitational number and it is also useful as it measures the relative importance of DEP and gravitational forces.

These numbers are given on figures 6. As expected, the Bond number which was greater but close to 1 highlights that the surface tension had a significant but not a dominant influence on the meniscus at the initial state. When the voltage increase, all the forces were first quite comparable until the DEP force became dominant compared to the surface tension force when the electric field exceeded $E \approx 2.13\,kV/mm$. The interface profiles of both fluids were still affected by gravity up to $E \approx 2.77\,kV/mm$. But beyond this value, both the electric bond number and the electrogravitational number Bo_E/Bo were greater than 10: the electric field strength made the DEP force fully dominant. The flat interface was thus produced by this force which erased the curving effect of surface tension even though the contact angle remains close to zero. However, following this reasoning, a flatter and flatter interface would be observable with the increase of the electric field and then, it is not possible to appreciate why the meniscus was still curved and tilted at intermediate voltage.

Free charges and the corresponding Coulomb force in the liquid could be an additional contribution influencing the interface profile. Actually, the weak electrical conduction in the liquid may generate a horizontal pressure gradient in the liquid which could consequently affect the interface profile. The bulk distribution of the dissociated ions can be identified based on the dimensionless number C_0 which is the ratio between the transit time $t_0 = D/(2\,bE)$ and the charge relaxation time $\tau = \varepsilon_l/(n_{eq}\,e\,2\,b)$:

$$C_0 = \frac{t_0}{\tau} = \frac{n_{eq}\,e\,D}{\varepsilon_l\,E} \tag{5}$$

where n_{eq} is the charge density of ions at dissociation/recombination equilibrium when no electric field is applied. For $C_0 \gg 1$ i.e. at low voltage for a given fluid, the quasi-ohmic conduction regime is established. The charges form two thin heterocharge layers located close to each electrode. The effect on liquid pressure is then limited as the liquid bulk largely remains electro-neutral. As the voltage increases, the layers gradually spread in the liquid. When $C_0 \leq 1$, the net charge (positive + negative charges) profile fills the inter-electrodes spacing entirely and, as a consequence, the liquid pressure gradient is fully affected by the Coulomb term.

The equilibrium densities were determined for both fluids using the voltage/current characteristic curves determined experimentally. Based on a one-dimensional model for the conduction in a dielectric liquid between parallel infinite electrodes [25], it can be demonstrated that the intersection point between the ohmic regime and the saturation asymptote on figure 3 is actually defined such as $C_0 = 1$. As a consequence, we have:

$$n_{eq} = \frac{\varepsilon_l\,U_s}{e\,D^2} \tag{6}$$

where U_s is the voltage at the intersection point. We found that $n_{eq} \approx 0.9\,10^{17} m^{-3}$ for HFE-7000 and $n_{eq} \approx 1.2\,10^{17} m^{-3}$ for HFE-7100. Therefore, C_0 was quite similar for both fluids in our experiments. For $D = 3.02\,mm$, it linearly decreased from $C_0 \approx 1$ at $E = 0.69\,kV/mm$ to $C_0 \approx 0.2$ at $E = 3.48\,kV/mm$. For $D = 2.03\,mm$, C_0 was 2/3 times smaller. Then, the conduction mainly corresponded to regimes in which free charges may impact the horizontal pressure profile in the liquid bulk entirely.

Following the same 1D approach used by Atten and Yagoobi [5] for the conduction regime, it could be demonstrated (see Appendix A) that, for the saturation regime, the horizontal pressure difference in the liquid between the electrodes and the

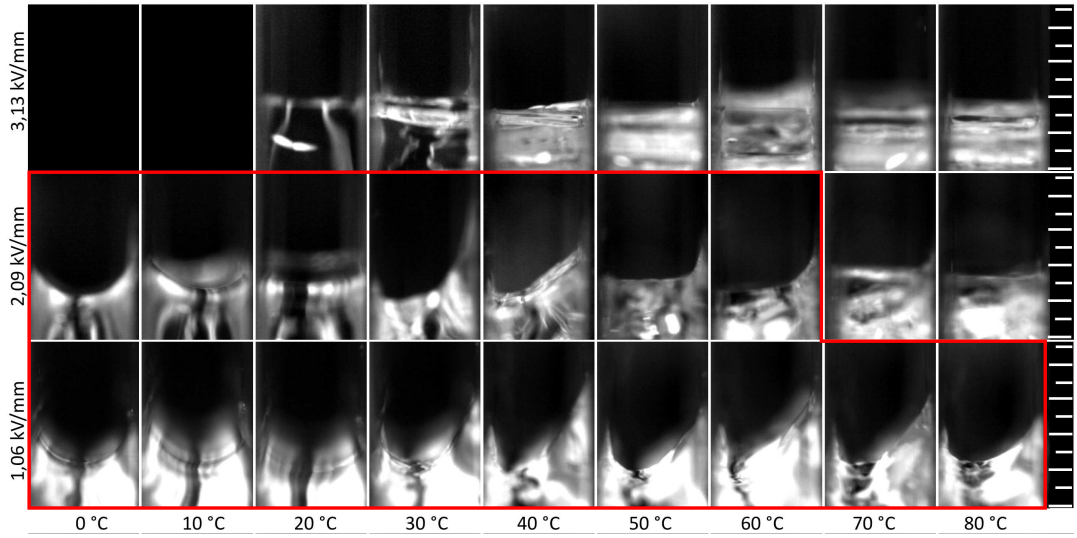

Figure 7: Interface profile on the operating range of temperature for HFE-7100; the HV electrode was on the right-hand side; the red line delimits the range in which the interface profile was significantly affected by the conduction in the liquid.

position from the HV electrode L (see equation A.2) of the zero net-charge vertical plane are:

- for the negative net charge layer close to the HV electrode,

$$\Delta p_{sat}^{HV} \approx \frac{n_{eq}^2\, e^2}{\varepsilon_l}\,\frac{D^2}{2}\,\frac{b^+}{b^-} \tag{7}$$

- for the positive net charge layer close to the ground electrode,

$$\Delta p_{sat}^{G} \approx \frac{n_{eq}^2\, e^2}{\varepsilon_l}\,\frac{D^2}{2}\,\frac{b^-}{b^+} \tag{8}$$

This shows that (i) without a significant field-enhanced dissociation, the horizontal pressure difference increases when the voltage increases and finally reaches a maximum value with no electric field dependency at the saturation regime, (ii) the asymmetry of the pressure profile between the electrodes is introduced by the ratio of the charge mobilities and actually, these relations verify that the pressure profile is symmetrical when $b^- = b^+$ as $\Delta p_{sat}^{HV} = \Delta p_{sat}^{G}$ and $L = D/2$.

A dimensionless number $Bo_{C,sat}$ is introduced in order to measure the relative influence of this horizontal pressure gradient on the interface profile. The capillary pressure is still used as the reference scale according to the relation (4):

$$Bo_{C,sat} = \frac{\frac{n_{eq}^2\, e^2}{\varepsilon_l}\,\frac{D^2}{2}}{\frac{2\gamma}{D}} = \frac{n_{eq}^2\, e^2\, D^3}{4\,\gamma\,\varepsilon_l} \tag{9}$$

Based on the equilibrium densities previously estimated, we found that $Bo_{C,sat} \approx 2$ for the HFE-7100 at $60°C$. This shows that the influence of the horizontal pressure gradient was comparable with surface tension and gravity at the initial state and with DEP force at low voltage. Then, the increase of the electric field made the DEP force dominant as the ratio $Bo_E/Bo_{C,sat}$ became greater than 10 when $E \geq 2.9\,kV/mm$. This is consistent with the fact that we observed a non-flat interface until this electric field strength. On top of that, a greater liquid height-of-rise in contact with the HV electrode suggested that for both fluids, the mobility of negative charges is somewhat lower than those of the positive ones. The influence of the space charge on the pressure gradient is increased by this effect according to equation (7).

Figure 7 shows the influence of the temperature on the meniscus shape for HFE-7100. No significant influence of the temperature was perceptible at the greatest electric field as the DEP force was fully dominant on the temperature range. At lower electric field strengths, as the Bond number was weakly affected, the analysis must rely on the temperature influence, (i) on the conduction structure in the liquid and (ii) on the relative importance of the DEP versus the electrical conduction.

Regarding the first point, we previously observed (figure 3) that the saturation regime was established for temperatures greater than 40°C. Below this temperature, the charges distribution at $E = 1.06\,kV/mm$ was close to those of the quasi-ohmic regime and then, the horizontal pressure drop in the liquid [5] was lower than Δp_{sat}. However, it could be significantly affected by field-enhanced dissociation at greater field and at low temperature. This is consistent with the observations where the interface profile was mostly affected by the electrical conduction for $T \geq 30°C$. At greater temperature, the relationship between Δp_{sat} and the temperature is then decisive.

We have seen that the dielectric constant was slightly affected by the temperature so that it can be assumed that Δp_{sat} mainly depends on the temperature variation of n_{eq}. Actually, this

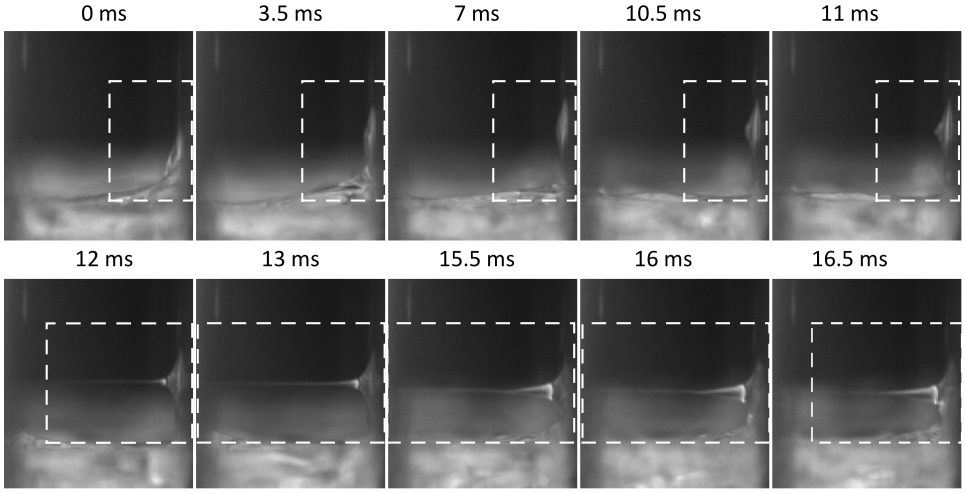

Figure 8: Formation and dynamics of a micro-jet close to the HV electrode wall at high electric field strength in HFE-7100.

could be estimated by the relationship between the charge mobility and the temperature considering that $n_{eq} = \sigma/(b^+ + b^-)$. [23] found that σ is a decreasing function of temperature within the operating range. Moreover, according to Walden's rule, the charge mobility depends on the inverse of the liquid viscosity which is divided by twice between 0°C and 80°C for the HFE-7100; so, when the temperature rises, the mobility of the ions could double and n_{eq} could significantly decrease with temperature. As a consequence, when the saturation regime is established, the effect of the conduction should decrease with an increase of temperature. On top of that, the relative importance of the DEP versus the electrical conduction should increase. This was actually noticeable for both low field strengths. At $E = 1.06\,kV/mm$, the effect of the DEP force was not really significant and the sole influence of the temperature on conduction could explain the slightly diminution of the asymmetry of the profile with increasing temperature. At $E = 2.09\,kV/mm$, the DEP force was almost 4 times greater so that the increase of the relative importance of the DEP with the temperature probably led to a flatter interface with temperature.

4.3. A charged interface behavior at the wall

Figure 8 shows a capture of one of some liquid jets regularly arising at high electric field in the interfacial region where the liquid accumulated along the HV electrode. The process started from the occurrence and the instability of a liquid film (0 to 7 ms). A deformation of this film into a micro-cone led to a horizontal cylindrical jet of liquid (11 ms) spreading along the electric field line. This jet was maintained between both electrodes until 15.5 ms and then returned to HV electrode until a new jet appeared. Sometimes, the jets broke in a Rayleigh-like instability to form some droplets.

The electrojet process is actually well-known. A review and detailed descriptions of the free surface instabilities in a electric field is given by Zhakin [26]. It is shown that this behavior typically concerns the electrodynamics of a charged surface in which both bulk and surface conductivities need to be considered (non-equipotential surface). As this process could significantly affect the structure of the interface, the occurrence of these instabilities may play a major role in deteriorating the control of the cooling system performance.

5. Conclusion

The effect of a DC electric field on a liquid-vapor interface was investigated at different temperatures using a Pellat-like test cell filled with HFE-7000 and HFE-7100 dielectric fluids.

The experimental results confirmed first that the DEP force controls the mean position of the meniscus as it compared quite favorably with the dielectric height-of-rise model. Moreover, the visualizations of the meniscus revealed that the DEP force could become locally so dominant compared to surface tension force so that the interface could be almost totally flattened when the electric field is increased.

These visualizations also revealed that the electrical conduction in the liquid could play a role in affecting, at the second order, the pressure profile in the liquid bulk. The modifications of the liquid horizontal pressure by the dissociation of ions have been determined on the basis of a 1D model of conduction for the saturation regime as most of our experiments were given by $C_0 \leq 1$. We demonstrated that the asymmetry of the profile could be due to a difference between the mobilities of positive and negative charges. An additional effect of the free charges was identified with the emergence of some interface instabilities leading to the formation of micro-jets close to the triple line. In our experiments, the electric field was mainly parallel to the interface and this phenomenon did not significantly perturb the interface position and its control. However, this may be an issue to consider for DC voltage and for a different electrodes configuration.

The effect of temperature of the interface behavior was quite weak and it was given by the temperature dependence of both the dielectric constant and ions mobilities when the electrical conduction was significant in the liquid. However, the temperature introduces a major drawback for cooling applications as

the interface control was mainly limited by the temperature dependence of the vapor dielectric strength which is highly sensitive to vapor pressure. As a consequence, a drastic limitation of the maximum electric field that the fluid can withstand before breakdown existed at low temperature and, finally, if the opportunity of using the EHD forces to control a liquid-vapor interface was confirmed, the temperature dependence for the vapor dielectric strength must be carefully considered in determining the working fluids which are suitable for EHD enhanced heat transfer applications.

Acknowledgment

Financial support from the French Research Agency, for EDYPHICE project undergrant number ANR-14-CE05-0031, is gratefully acknowledged.

Nomenclature

Symbol, definition, SI units

b	Ionic mobility, $m^2/(Vs)$
c	Neutral species density, $/m^3$
D	Inter-electrodes spacing, m
e	Electron charge, C
E	Electric field strength, V/m
f	Force by unit of volume, N/m^3
g	Gravitational acceleration, m/s^2
h	Liquid height-of-rise, m
K_r	Recombinaison rate coefficient m^3/s
K_d	Dissociation rate coefficient, $1/s$
p	Pressure, Pa
n	Ionic density, $/m^3$
q	Net charge volume density, C/m^3
t	Time, s
V	Electrical potential, V
x	Space coordinate, m

Greek symbols

ε	Permittivity, F/m
ε_r	Dielectric constant
γ	Surface tension, N/m
ρ	Mass density, kg/m^3
σ	Electrical conductivity, S/m

Subscripts

0	vacuum
eq	equilibrium state
l	liquid
sat	saturation regime
v	vapor

Superscripts

$+$	positive charge
$-$	negative charge
HV	high voltage electrode
G	ground electrode

Appendix A. Effect of pure conduction on the pressure in a liquid dielectric between two infinite parallel plane electrodes when $C_0 \ll 1$

Thomson and Thomson [25] proposed a model for pure conduction in a dielectric medium in which (i) the processus of charge creation is only due to dissociation/recombination (ii) the charge diffusion is not significant compared to ions drift and (iii) no medium motion takes place. These developments have been reproduced for $C_0 \gg 1$ in Atten and Yagoobi [5]. In the $C_0 \ll 1$ case, it was shown that an approximate solution is given by neglecting the recombination in the bulk entirely. Assuming a constant dissociation rate and satisfying the boundary conditions at the the electrodes i.e. $n^+(0) = 0$ (the HV electrode is located in $x = 0$) and $n^-(D) = 0$, it was demonstrated that the Coulomb body force and thus the horizontal pressure gradient in the liquid is a linear function of space:

$$\frac{\partial p}{\partial x} = (n^+ - n^-)\, e\, E = K_d\, c_{eq}\, e \left(\frac{1}{b^+} + \frac{1}{b^-}\right) x - \frac{K_d\, c_{eq}\, e}{b^-}\, D \quad \text{(A.1)}$$

where n^+ is the charge density of positive ions, n^- is the charge density of negative ions, E is the local field strength, K_d the rate of dissociation, c_{eq} is the constant concentration of neutral species, b^+ and b^- are respectively the charge mobilities of positive and negative ions.

The horizontal pressure in the liquid is then parabolic and the maximum pressure difference is established between the wall and the vertical plane such as the net charge $q = (n^- - n^-)\, e = 0$ (see figure A.9). Using the previous equation, the position (from the HV electrode) $x = L$ of this plane is given by:

$$L = \frac{\frac{b^+}{b^-}}{1 + \frac{b^+}{b^-}}\, D \quad \text{(A.2)}$$

Integrating the equation A.1 between $x = L$ and the high voltage position x, the pressure difference between both positions is:

$$\Delta p^{HV} = p(0) - p(L) = K_d\, c_{eq}\, e \left(\frac{b^+}{b^-}\right) \frac{1}{(b^+ + b^-)}\, \frac{D^2}{2} \quad \text{(A.3)}$$

In a similar way, the pressure difference between the grounded electrode and $x = L$ is:

$$\Delta p^{G} = p(D) - p(L) = K_d\, c_{eq}\, e \left(\frac{b^-}{b^+}\right) \frac{1}{(b^+ + b^-)}\, \frac{D^2}{2} \quad \text{(A.4)}$$

At equilibrium (when no electric field is applied), we have $n_{eq} = n^+_{eq} = n^-_{eq}$ and $K_{d,eq}\, c_{eq} - K_r\, n^2_{eq} = 0$ in which the recombination constant is given by Langevin relation $K_r = (b^+ + b^-)\, e/\varepsilon_l$. Assuming that the rate of dissociation is not significantly affected by the electric field i.e. $K_d \approx K_{d,eq}$, we finally obtained:

- close to the HV electrode,

$$\Delta p_{sat}^{HV} \approx \frac{n_{eq}^2\, e^2}{\varepsilon_l}\,\frac{D^2}{2}\,\frac{b^+}{b^-} \tag{A.5}$$

- close to the ground electrode,

$$\Delta p_{sat}^{G} \approx \frac{n_{eq}^2\, e^2}{\varepsilon_l}\,\frac{D^2}{2}\,\frac{b^-}{b^+} \tag{A.6}$$

Coulomb body force and pressure profiles deduced from this analysis are given in Figure A.9.

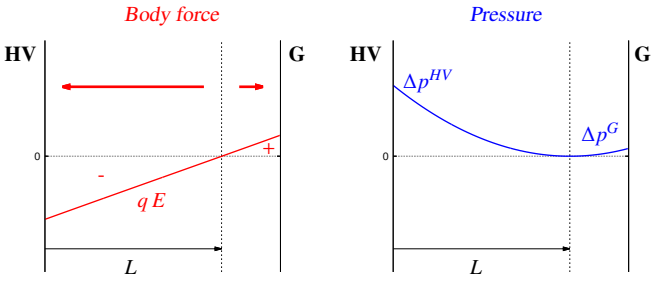

Figure A.9: Coulomb body force and pressure profiles in liquid at saturation regime when the mobility of positive ions is greater than those of the negative ions.

References

[1] T. B. Jones, Electrohydrodynamic heat pipes, International Journal of Heat and Mass Transfer 16 (1972) 1045–1048.

[2] T. Jones, M. Perry, Electrohydrodynamic heat pipe experiments, Journal of Applied Physics 45 (5) (1974) 2129–2132.

[3] R. I. Loehrke, W. J. Day, Performance characteristics of several ehd heat pipe designs, Journal of Electrostatics 5 (1978) 285–296.

[4] B. R. Babin, G. P. Peterson, J. Seyed-Yagoobi, Experimental investigation of an ion-drag pump-assisted capillary loop, Journal of Thermophysics and Heat Transfer 7 (2) (1993) 340–345.

[5] P. Atten, J. Seyed-Yagoobi, Electrohydrodynamically induced dielectric liquid flow through pure conduction in point/plane geometry, IEEE Transactions on Dielectrics and Electrical Insulation 10 (1) (2003) 27–36.

[6] J. E. Bryan, J. Seyed-Yagoobi, Heat transport enhancement of monogroove heat pipe with electrohydrodynamic pumping, Journal of Thermophysics and Heat Transfer 11 (3) (1997) 454–460.

[7] S.-I. Jeong, J. S. Yagoobi, Experimental study of electrohydrodynamis pumping through conductino phenomenon, Journal of Electrostatics (2002) 123–133.

[8] M. R. Pearson, J. Seyed-Yagoobi, Experimental study of linear and radial two-phase heat transport devices driven by electrohydrodynamic conduction pumping, Journal of Heat Transfer 137 (2015) 1–9.

[9] V. K. Patel, J. Seyed-Yagoobi, Combined Dielectrophoretic and Electrohydrodynamic Conduction Pumping for Enhancement of Liquid Film Flow Boiling, Journal of Heat Transfer-Transactions of the ASME 139 (6).

[10] S.-I. Jeong, J. Didion, Thermal control utilizing an electrohydrodynamic conduction pump in a two-phase loop with high heat flux source, Journal of Heat Transfer 129 (2007) 1576–1583.

[11] S.-I. Jeong, J. Didion, Performance characteristics of electrohydrodnamic conduction pump in two-phase loops, Journal of Thermophysics and Heat Transfer 22 (1) (2008) 90–97.

[12] B. Mo, M. M. Ohadi, S. V. Dessiatoun, K. H. Cheung, Startup time reduction in an electrohydrodynamically enhanced capillary pumped loop, Journal of Thermophysics and Heat Transfer 13 (1) (1999) 134–139.

[13] B. Mo, M. M. Ohadi, S. V. Dessiatoun, K. R. Wrenn, Capillary pumped-loop thermal performance improvement with electrohydrodynamic technique, Journal of Thermophysics and Heat Transfer 14 (1) (2000) 103–108.

[14] G. D. Harvel, B. Komeili, C. Y. Ching, J.-S. Chang, Electrohydrodynamically enhanced capillary evaporator, IEEE Transactions on Dielectrics and Electrical Insulation 16 (2) (2009) 456–462.

[15] S. Laohalertdecha, P. Naphon, S. Wongwises, A review of electrohydrodynamic enhancement of heat transfer, Renewable and Sustainable Energy Reviews 11 (2007) 858–876.

[16] K. Smith, G. Byrne, R. Kempers, A. J. Robinson, Electrohydrodynamic augmentation of a reflux thermosyphon, Experimental Thermal and Fluid Science 79 (2016) 175–186.

[17] M. Bazant, R. Bennewitz, L. Bocquet, N. Brilliantov, R. Dey, C. Drummond, R. Dryfe, H. Girault, K. Hatzell, K. Kornev, A. A. Kornyshev, I. Kratochvilova, A. Kucernak, M. Kulkarni, S. Kumar, A. Lee, S. Lemay, H. Medhi, A. Mount, F. Mugele, S. Perkin, M. Rutland, G. Schatz, D. Schiffrin, E. Smela, E. Smirnov, M. Urbakh, A. Yaroshchuk, Electrotunable wetting, and micro- and nanofluidics: general discussion, Faraday Discussions 199 (2017) 195–237.

[18] H. Pellat, Mesure de la force agissant sur les diélectriques liquides non électrisés placés dans un champ électrique, C. R. de l'Académie des Sciences de Paris 119 (1895) 691–694.

[19] W. Welters, L. Fokkink, Fast electrically switchable capillary effects, Langmuir 14 (7) (1998) 1535–1538.

[20] T. B. Jones, K.-L. Wang, D.-J. Yao, Frequency-dependent electromechanics of aqueous liquids :electrowetting and dielectrophoresis, Langmuir 20 (2004) 2813–2818.

[21] T. B. Jones, R. Gram, K. Kentch, D. R. Harding, Capillarity and dielectrophoresis of liquid deuterium, Journal of Physics D-Applied Physics 42 (22).

[22] L. Onsager, Deviation from ohm's law in weak electrolytes, Journal of Chemical Physics 2 (1934) 599–615.

[23] M. Nassar, C. Louste, A. Michel, M. Daaboul, Experimental investigation of the variation of HFE electric properties with temperature, 2018, proc. Electrostatics Joint Conference, Boston, USA, 18-20 June.

[24] M. H. Rausch, L. Kretschmer, S. Will, A. Leipertz, A. P. Froeba, Density, Surface Tension, and Kinematic Viscosity of Hydrofluoroethers HFE-7000, HFE-7100, HFE-7200, HFE-7300, and HFE-7500, Journal of Chemical and Engineering Data 60 (12) (2015) 3759–3765.

[25] J.-J. Thomson, G. P. Thomson, Conduction of electricity through gases, Cambridge University Press, 1928.

[26] A. I. Zhakin, Electrohydrodynamics of charged surfaces, Physics-Uspekhi 56 (2) (2013) 141–163.